

Enhancing the Efficiency of MEH-PPV and PCBM Based Polymer Solar Cells Via Optimization of Device Configuration and Processing Conditions

En Chung Chang,¹ Ching-Ian Chao,¹ Rong-Ho Lee²

¹Opto-Electronics and Systems Laboratories, Industrial Technology Research Institute, Hsinchu, Taiwan 310, Republic of China

²Department of Chemical Engineering, National Yunlin University of Science and Technology, Yunlin, Taiwan 640, Republic of China

Received 24 August 2005; accepted 2 November 2005

DOI 10.1002/app.23657

Published online in Wiley InterScience (www.interscience.wiley.com).

ABSTRACT: Polymer solar cells were fabricated based on an interpenetrated network of conjugated polymer poly(2-methoxy-5-(2'-ethyl-hexyloxy)-1,4-phenylenevinylene) (MEH-PPV) as electron donor and fullerene derivative (6,6)-phenyl-C₆₁-butyric acid methyl ester (PCBM) as electron acceptor. The photovoltaic performances were strongly dependent on the surface treatment of anode, conductivity of hole-transporting material, the thickness of MEH-PPV:PCBM composite film, and the cathode configuration. Best photovoltaic performances were obtained for the solar cell constructed with O₂ plasma-treated anode glass, high conductivity hole-transporting material PEDOT, photoactive film

thickness of 180 nm, and calcium/silver cathode. Open circuit voltage of 0.79 V, short circuit current density of 4.79 mA/cm², fill factor of 44.4%, and 2.07% power conversion efficiency were obtained for the solar cell under 80 mW/cm² white light from a halogen lamp. The influences of device fabrication conditions and configuration on the photovoltaic performance of MEH-PPV:PCBM composite film-based polymer solar cells were discussed in detail. © 2006 Wiley Periodicals, Inc. *J Appl Polym Sci* 101: 1919–1924, 2006

Key words: polymer solar cell; photovoltaic cell; MEH-PPV; PCBM

INTRODUCTION

Development of efficient solar cells is considered one of the new approaches to pursue inexpensive renewable energy sources. Organic solar cells are a promising alternative to conventional inorganic solar cells because of the advantages of large area, flexible shape, light weight, easy processing, and low cost fabrication. The photovoltaic effects of the organic materials based solar cells have been studied extensively, including dye sensitized,^{1–4} small molecular,^{5,6} organic/inorganic hybrid,^{7,8} and conjugated polymer/inorganic^{9,10} based solar cells.

The major advance in solar energy conversion efficiency has been accomplished replacing the bilayer device with the bulk heterojunction configuration for the photoactive layer.^{9,11–13} Unlike the bilayer device, the bulk heterojunction is able to circumvent the limitation of the charge generation at a two-dimensional network of photoinduced charge generating interfaces. The improvement of the bulk heterojunction

configuration lies in enhancing the solid state morphology of conjugated polymer/fullerene derivative blend, which results in higher power conversion efficiency of the polymer solar cell.^{9,11–13} Therefore, the photoactive layer of organic solar cells based on conjugated polymer/fullerene derivative blends, such as poly(2-methoxy-5-(2'-ethylhexyloxy)-1,4-phenylenevinylene) and [6,6]-phenyl C₆₁ butyric acid methyl ester (MEH-PPV:PCBM), have been studied extensively over the past few years.^{11,12,14,15}

In addition to the morphology of the photoactive layer, the device processing condition and configuration also play an important role on the photovoltaic performance of polymer solar cell. The plasma treatment of the anode surface leads to the high value of ITO work function and enhancement of hole injection at the interface of indium tin oxide (ITO) and hole-transporting layer (HTL).^{16–20} The insertion of the hole transporting material (HTM) between ITO and photoactive layer brings about the enhancement of the open circuit voltage of the polymer solar cell.¹¹ For the conjugated polymer/PCBM based solar cell, the morphology of the polymer blend and photovoltaic effect were directly related to the concentration and solubility of electron acceptor PCBM in the casting solvent.^{11,13,21} Brabec and coworkers have reported that the chlorobenzene-cast photoactive layer shows

Correspondence to: R.-H. Lee (lerongho@yuntech.edu.tw).

Contract grant sponsor: National Science Council of Taiwan; contract grant number: NSC93-2622-E-224-018-CC3.

nearly threefold value of power conversion efficiency than the cell produced from toluene.¹³ It is attributed to the fact that the better solubility of PCBM in chlorobenzene was obtained as compared to that in toluene. Moreover, the open circuit voltage in polymer solar cells was strongly dependent on the electron acceptor strength of the fullerene derivative.²² In addition, the cathode effect on the photovoltaic performance has also been studied for the conjugated polymer/PCBM based solar cell.^{11,22,23} Brabec et al. have reported that higher fill factor and power conversion efficiency were obtained for the cell with LiF interfacial layer as compared to the cell without LiF layer.²³

The influences of device processing condition and configuration on the photovoltaic performance have been studied for the conjugated polymer/PCBM based solar cell. However, the anode surface pretreatment, HTL, morphology of photoactive layer, and cathode configuration effects on the photovoltaic performance have not been examined thoroughly. In this study, the systematic optimization of polymer solar cells with MEH-PPV : PCBM composite film was attempted. The effect of anodic surface treatment on the photovoltaic performance was carried out for the polymer solar cells treated with oxygen, nitrogen, and Ar-plasma, respectively. The optimized thin film processing condition was determined by the performance evaluation of polymer solar cells with different photoactive layer thicknesses. Polymer solar cells with different cathode configurations, such as Ag, Al, Ca/Ag, and LiF/Al cathodes have been investigated for the cathode effect on the photovoltaic behavior. The photovoltaic performances of MEH-PPV : PCBM composite film-based solar cells would be enhanced through the aforementioned optimization of processing conditions and device configuration (Fig. 1).

EXPERIMENTAL

The polymer solar cells were fabricated based on an interpenetrated network of conjugated polymer MEH-PPV and fullerene derivative PCBM. The MEH-PPV was purchased from ADS (American Dye Source, Canada; $M_n = 320,000$), and PCBM was used as received from Prof. Y. Yang's Lab of UCLA. The HTM PEDOT/PSS (Baytron P CH8000 and Baytron P AI4083) was purchased from Bayer. Solutions of the conjugated polymer MEH-PPV and PCBM were prepared with 1,2-dichlorobenzene (3 wt %) in the optimized weight ratio of 1 : 4.¹³ The substrate of polymer solar cells was an ITO-coated glass with a sheet resistance of 15 Ω /sq (Applied Film). The calcium was purchased from Furuuchi Chemical (CAM-2002A, Japan; 99.5%). The polymer solar cells were prepared according to the following procedure. Glass substrates with patterned ITO electrodes were well washed and

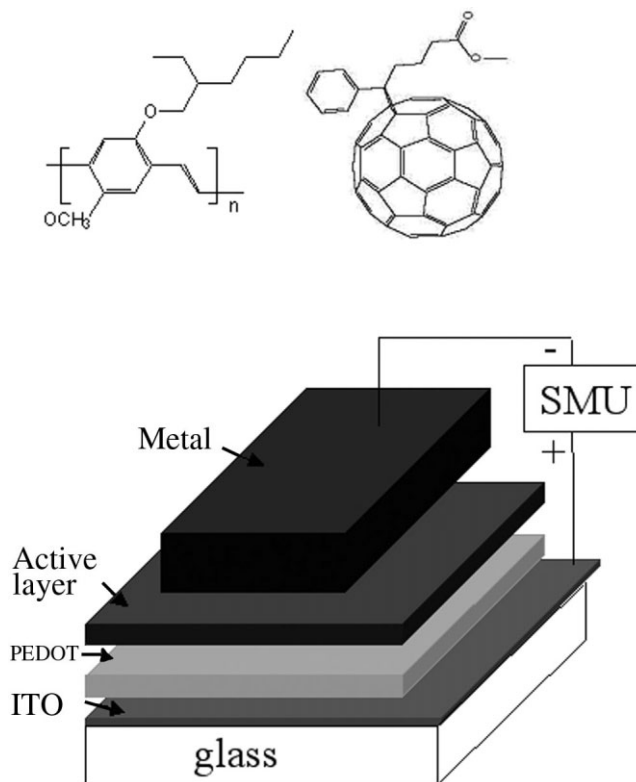


Figure 1 Chemical structure and device configuration of MEH-PPV and PCBM-based polymer photovoltaic cell.

cleaned by O_2 , N_2 , or Ar-Plasma treatment. The thin film of HTM PEDOT (Baytron P CH8000 and Baytron P AI4083, Bayer) was formed on the ITO layer of a glass substrate by the spin-casting method. The MEH-PPV and PCBM-based photoactive film was spin-coated from the 1,2-dichlorobenzene solution onto the PEDOT layer and was dried at 80°C for 1 h in a glove box. A high purity aluminum, silver, Ca/Ag, or LiF/Al-based cathode was thermally deposited onto the MEH-PPV and PCBM-based photoactive thin film in a high vacuum chamber. The active area of the photovoltaic cell is 0.04 cm^2 . After the electrode deposition, the polymer solar cell was transferred from the evaporation chamber to a glove-box purged by high purity nitrogen gas to keep oxygen and moisture levels below 1 ppm. The cell was then encapsulated by glass covers, which was sealed with UV-cured epoxy glue in the glove box. The deposition rate of cathode was determined with a quartz thickness monitor (STM-100/MF, Sycon). The thickness of the thin film was determined with a surface texture analysis system (3030ST, Dektak). The current density-voltage (J-V) characteristics of the polymer solar cell were measured on a programmable electrometer with current and voltage sources (Keithley 2400) under an illumination of 80 mW/cm^2 (AM 1.5 solar simulator corrected) white light from a halogen lamp.

RESULTS AND DISCUSSION

The influences of device fabrication conditions and configuration on the performance of MEH-PPV : PCBM-based polymer solar cells were discussed as follows:

Plasma treatment effect on anodic surface

The treatment of the ITO surface is important for the improvement of photovoltaic cell performance due to the reduction of hole injection energy barrier, and the enhancement of hole injection at the interface of ITO and hole-transporting layer.^{16–20} The current density versus voltage characteristic of polymer solar cells containing different plasma-treated ITO substrates is shown in Figure 2. The values of photovoltaic performances, such as open circuit voltage (V_{oc}), short circuit current density (I_{sc}), fill factor (FF), and power conversion efficiency (η), are also given in the inset of Figure 2. The thickness of the MEH-PPV : PCBM-based photoactive layer was 180 nm. The result indicates that the solar cell with O_2 -plasma-treated ITO substrate exhibits the better photovoltaic performance than the cells with N_2 and Ar-plasma-treated substrates. High value of open circuit voltage was obtained for the cell with O_2 -plasma-treated ITO substrate. Values of the fill factor and power conversion efficiency of the O_2 -plasma-treated cell were similar to those of the one treated with N_2 plasma. Ar-plasma-treated cell exhibits the poorest photovoltaic performance among all the plasma-treated cells. This result implies that the enhancement of the ITO work function was more significant for the O_2 -plasma-treated ITO substrate in comparison with the other plasma-treated cells. Moreover, the plasma treatment effect on

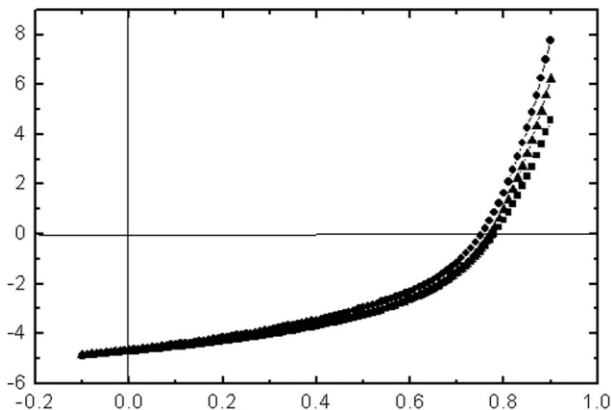


Figure 2 Current density versus voltage characteristic of photovoltaic cell with different plasma-treated anode substrate; device configuration: ITO/(O_2 , N_2 , and Ar Plasma)/PEDOT(AI4083)/MEH-PPV : PCBM/Ca/Ag; Photovoltaic parameters are given in the inset: V_{oc} in V, I_{sc} in mA/cm².

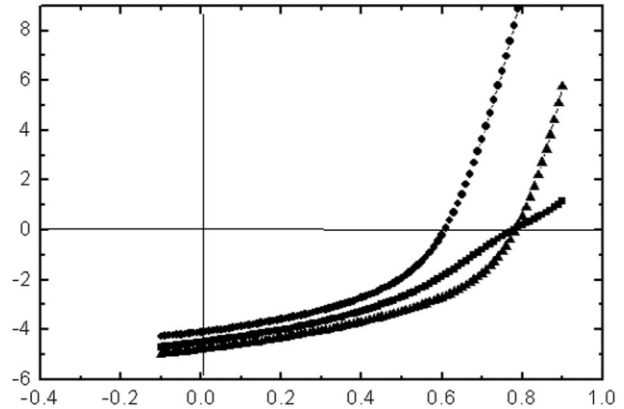


Figure 3 Current density versus voltage characteristic of photovoltaic cell with different hole-transporting materials; device configuration: ITO/PEDOT(CH8000, CH8000/HT1100, AI4083, X)/MEH-PPV : PCBM/Ca/Ag; Photovoltaic parameters are given in the inset: V_{oc} in V, I_{sc} in mA/cm².

the open circuit voltage was more pronounced than the short circuit current density. This is due to the fact that the open circuit voltage was dominantly determined by the work function of ITO and HOMO value of HTL.¹¹ The value of short circuit current density was directly related to the electron injection barrier and serial resistivity of polymer-based photoactive layer.

Hole-transporting layer effect on photovoltaic performance

The HTM PEDOT has been widely used to improve the brightness, efficiency, and operation stability of polymer emitting devices, due to the high HOMO value of PEDOT, and the improvement of the ITO surface roughness and interface contact between ITO and light emitting polymer film.^{24–27} Similarly, the PEDOT has also been used as the HTM for the polymer solar cell.¹¹ Despite that the PEDOT effect on the photovoltaic performances has been studied,¹¹ the conductivity effect of PEDOT on the photovoltaic performances has not yet been investigated. Two PEDOT materials with different conductivity (CH8000: $\sim 10^5 \Omega \cdot \text{cm}$ and AI4083: $\sim 10^3 \Omega \cdot \text{cm}$) were used to study the hole-transporting effect on photovoltaic performance. The current density versus voltage characteristic of photovoltaic cells with or without different hole-transporting layers (CH8000 and AI4083) is shown in Figure 3. The thickness of the MEH-PPV : PCBM-based photoactive layer was 180 nm. The photovoltaic cell containing PEDOT CH8000 (60 nm) as HTL exhibited better photovoltaic performance as compared to the cell without PEDOT. The interfacial PEDOT layer at the anode led to an increase in the open circuit voltage. It is attributed to the high work function of PEDOT (~ 5.2 eV) with respect to that of ITO (4.4–4.7

eV).¹¹ In addition to the open circuit voltage, the short circuit current density was also increased with the insertion of HTL, which was not mentioned previously.¹¹ This result demonstrates that the PEDOT was capable of facilitating the hole transporting and collecting processes at the anode of the photovoltaic cell. As a result, a higher short circuit current density was obtained for the HTL-containing cell. High open circuit voltage and short circuit current density would certainly result in the low fill factor and high power conversion efficiency for the cell with HTL. Moreover, the cell with the high conductivity PEDOT AI4083 (80 nm) exhibited better photovoltaic performance than the cell with the low conductivity PEDOT CH8000. The value of open circuit voltage was not increased with increasing PEDOT conductivity. This is due to the fact that the PEDOT CH8000 and AI4083 possess similar HOMO values. High conductivity PEDOT would also promote the hole transporting and collecting processes at the anode of photovoltaic cell. As a result, a higher short circuit current density was obtained for the cell with the PEDOT AI4083 layer. Furthermore, the cell with high conductivity HTL exhibits a lower serial resistivity, which is responsible for the increase of the fill factor and power conversion efficiency.²³ From the aforementioned information, the best photovoltaic performance was obtained for the cell containing high conductivity HTL. The conductivity of HTM plays an important role in the photovoltaic performance of MEH-PPV : PCBM-based polymer solar cell.

The thickness effect of polymer photoactive film

For the polymer photovoltaic cell, the photoactive layer of MEH-PPV : PCBM would absorb solar light and subsequently excite electron-hole pair. The electron-hole pair split into electron and hole would reach the cathode and anode, respectively, and generate current under the applied electron field. The photovoltaic performance is closely related to the thickness of photoactive layer. To study the thickness effect on the photovoltaic performance, the polymer solar cell with different photoactive layer thicknesses were fabricated. Current density versus voltage characteristics of photovoltaic cell with different photoactive layer thicknesses is shown in Figure 4. The thicknesses of MEH-PPV and PCBM-based photoactive layers are ranged from 130 to 210 nm. The open circuit voltage of the polymer solar cell was independent on the thickness of photoactive layer. The 0.79 V of open circuit voltage was obtained for the photovoltaic cells with different photoactive layer thicknesses. The open circuit voltage was mainly determined by the hole injection energy barrier at the interface of ITO and hole-transporting layer.¹¹ The short circuit current density was increased with increasing thickness of photoac-

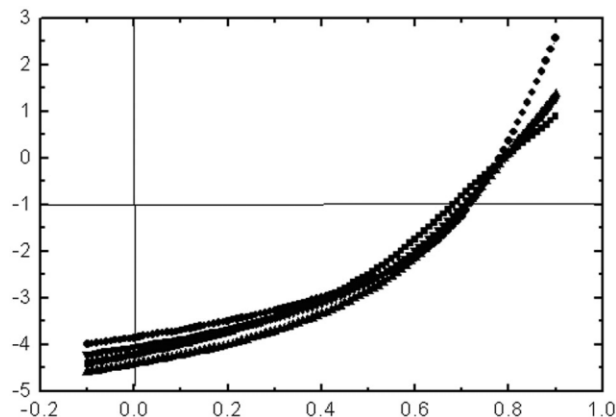


Figure 4 Current density versus voltage characteristic of photovoltaic cell with different photoactive layer thickness; device configuration: ITO/PEDOT(CH8000)/MEH-PPV : PCBM/Ca/Ag; Photovoltaic parameters are given in the inset: V_{oc} in V, I_{sc} in mA/cm^2 .

tive layer. A maximal short circuit current density with a thickness of 180 nm was obtained. This is due to the fact that a stronger absorption of solar light was obtained for the photovoltaic cell with a thicker photoactive layer. As a result, a higher short circuit current density was obtained. However, the fill factor was decreased with increasing thickness of photoactive layer. The value of fill factor was closely related to the serial resistivity of photovoltaic cell. The thicker photoactive layer leads to the higher resistance, and results in a lower fill factor of cell.²⁸ Moreover, a maximal power conversion efficiency (1.78%) with a thickness of 180 nm was obtained. The short circuit current density, fill factor, and power conversion efficiency were decreased as the photoactive layer thickness further increased up to 210 nm. Upon increasing the thickness of the photoactive layer, the factor of serial resistivity becomes dominant and consequently the short circuit current density breaks down because of the low mobility of charge carrier.²⁹ This also results in the reduction of the fill factor and power conversion efficiency. In addition to the lower charge mobility, the restriction of exciton diffusion distance leads to the low power conversion efficiency of solar cell with thick MEH-PPV : PCBM composite film.⁹

Cathode configuration effect on photovoltaic performance

To study the cathode configuration effect on the photovoltaic performance, the cells with different cathodes, including the Al, LiF/Al, Ag, and Ca/Ag metals were studied. Current density versus voltage characteristic of photovoltaic cells containing different cathode configuration is shown in Figure 5. The PEDOT AI4083 was used as the hole-transporting layer for the photovoltaic cells, whereas the thickness of the MEH-

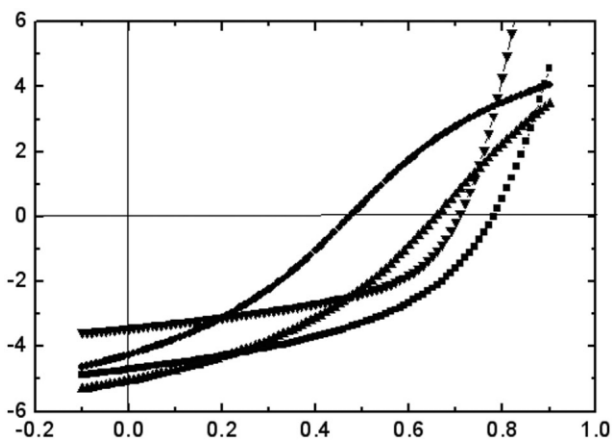


Figure 5 Current density versus voltage characteristic of photovoltaic cell with different metal-based cathodes; device configuration: ITO/PEDOT(AI4083)/MEH-PPV : PCBM/Metal (Ca/Ag, Ag, LiF/Al, and Al); Photovoltaic parameters are given in the inset: V_{oc} in V, I_{sc} in mA/cm^2 .

PPV : PCBM-based photoactive layer was 180 nm. The result indicates that the photovoltaic cell with LiF/Al cathode exhibited higher values of open circuit voltage, fill factor, and power conversion efficiency than the cell with Al cathode. Moreover, a higher current density was obtained for the cell with LiF/Al cathode, even through the short circuit current density of cell with LiF/Al cathode was slightly smaller than one with Al cathode. In particular, the current density decreased significantly with increasing voltage close to 0.47 V while the cell with Al cathode was utilized. The serial resistivity of the cell was reduced upon the insertion of a thin LiF layer between the photoactive layer and aluminum. This reduction of the serial resistivity is responsible for the increase of the fill factor and power conversion efficiency due to the formation of a better ohmic contact.²³ Brabec et al. have reported that the fill factor and power conversion efficiency of the cell with LiF interfacial layer increased by over $\sim 20\%$ as compared to those of the cell without LiF layer.²³ In this work, the pronounced enhancement of the open circuit voltage and fill factor was over 44%, whereas the power conversion efficiency was over 70%. In addition, the photovoltaic cell with Ag cathode exhibited a better photovoltaic performance than the cell with Al cathode did. This is due to the fact that the Ag cathode (4.26 eV) possesses a lower work function than the Al cathode (4.28 eV) does.²² The cathode with low work function was more favorable to the injection of electron into cathode. Furthermore, the performance of photovoltaic cell with Ca/Ag was better than the cell with Ag cathode. The electrode property was improved upon insertion of a Ca interfacial layer between photoactive layer and Ag. The cell with Ca/Ag cathode exhibits higher open circuit voltage, short circuit current density, and power conversion

efficiency as compared to the cell with LiF/Al cathode. This demonstrates that the Ca/Ag formed a better ohmic contact with the photoactive layer than the LiF/Al-based cathode did. The polymer solar cell with Ca/Ag cathode shows the best performance than the cell with other cathodes. The cathode configuration effect on polymer solar cell is similar to that on the polymer light emitting device.³⁰ The polymer light emitting device with Ca/Ag cathode shows higher current density and luminescence intensity than the devices with respective LiF/AL, Ag, and Al cathodes. It is concluded that the performance of the MEH-PPV:PCBM-based polymer solar cell was strongly dependent on the cathode configuration.

CONCLUSIONS

The influences of device processing conditions and device configuration on the photovoltaic performance of MEH-PPV : PCBM composite film-based polymer solar cells were investigated in this study. The photovoltaic performance was strongly dependent on the factors such as the surface treatment of anode, conductivity of hole-transporting material, the film thickness of MEH-PPV : PCBM composite film, and the cathode configuration. The solar cell with O_2 -plasma-treated ITO substrate shows better photovoltaic performance than the cells with N_2 and Ar-plasma-treated substrates. The plasma treatment effect on the open circuit voltage was more pronounced than that on the short circuit current density. Moreover, high conductivity PEDOT was favorable for facilitating the hole transporting and collecting processes at the anode of polymer solar cell. As a result, excellent performance was obtained for the cell with high conductivity PEDOT. In addition, the photovoltaic performance was also dependent on the thickness of MEH-PPV : PCBM composite film. A maximal power conversion efficiency ($\eta = 2.07\%$) with a thickness of 180 nm was obtained. The photovoltaic performance of the polymer solar cell was directly related to the cathode configuration. The cell with Ca/Ag cathode shows better performance than the cell with other cathodes (LiF/Al, Al, and Ag). In a nutshell, the photovoltaic performance of MEH-PPV : PCBM composite film-based polymer solar cells would be enhanced through the aforementioned optimization of processing conditions and device configuration.

The authors thank Prof. Y. Yang of UCLA for providing PCBM.

References

1. Oregan, B.; Gratzel, M. *Nature* 1991, 353, 737.
2. Bach, U.; Lupo, D.; Comte, P.; Moser, J. E.; Weissortel, F.; Salbeck, J.; Spreitzer, H.; Gratzel, M. *Nature* 1998, 395, 583.

3. Tachibana, Y.; Hara, K.; Sayama, K.; Arakawa, H. *Chem Mater* 2002, 14, 2527.
4. Gebeyehu, D.; Brabec, C. J.; Sariciftci, N. S. *Thin Solid Films* 2002, 403, 271.
5. Schon, J. H.; Kloc, C.; Batlogg, B. *Appl Phys Lett* 2000, 77, 2473.
6. Hansel, H.; Zettl, H.; Krausch, G.; Schmitz, C.; Kisselev, R.; Thelakkat, M.; Schmidt, H. W. *Appl Phys Lett* 2002, 81, 2106.
7. Yoo, S.; Domercq, B.; Kippelen, B. *Appl Phys Lett* 2004, 85, 5427.
8. Simon, P.; Maennig, B.; Lichte, H. *Adv Funct Mater* 2004, 14, 669.
9. Yu, G.; Gao, J.; Hummelen, J. C.; Wudl, F.; Heeger, A. J. *Science* 1995, 270, 1789.
10. Halls, J. J. M.; Pichler, K.; Friend, R. H.; Moratti, S. C.; Holmes, A. B. *Appl Phys Lett* 1996, 68, 3120.
11. Alem, S.; Bettignies, R. D.; Nunzi, J. M.; Cariou, M. *Appl Phys Lett* 2004, 84, 2178.
12. Jain, S. C.; Aernout, T.; Kapoor, A. K.; Kumar, V.; Geens, W.; Poortmans, J.; Mertens, R. *Synth Met* 2005, 148, 245.
13. Shaheen, S. E.; Brabec, C. J.; Sariciftci, N. S. *Appl Phys Lett* 2001, 78, 841.
14. Heller, C. M.; Campbell, I. H.; Smith, D. L.; Barashkov, N. N.; Ferraris, J. P. *J Appl Phys* 1997, 81, 3227.
15. Zhang, F.; Johansson, M.; Andersson, M. R.; Hummelen, J. C.; Inganas, O. *Adv Mater* 2002, 14, 662.
16. Kim, J. S.; Granstrom, M.; Friend, R. H.; Johansson, N.; Salaneck, W. R.; Daik, R.; Feast, W. J.; Cacialli, F. *J Appl Phys* 1998, 84, 6859.
17. Kim, J. S.; Friend, R. H.; Cacialli, F. *Appl Phys Lett* 1999, 74, 3084.
18. Kim, J. S.; Cacialli, F.; Cola, A.; Gigli, G.; Cingolani, R. *Appl Phys Lett* 1999, 75, 19.
19. Low, B.; Zhu, F.; Zhang, K.; Chua, S. *Appl Phys Lett* 2002, 80, 4659.
20. Utsumi, M.; Matsukaze, N.; Kumagai, A.; Shiraishi, Y.; Kawamura, Y.; Furusho, N. *Thin Solid Films* 2000, 363, 13.
21. Mihailetschi, V. D.; Koster, L. J. A.; Blom, P. W. M.; Melzer, C.; Boer, B. D.; Duren, J. K. J. V.; Janssen, R. A. J. *Adv Funct Mater* 2005, 15, 795.
22. Brabec, C. J.; Cravino, A.; Meissner, D.; Sariciftci, N. S.; Fromherz, T.; Rispens, M. T.; Sanchez, L.; Hummelen, J. C. *Adv Funct Mater* 2001, 11, 374.
23. Brabec, C. J.; Shaheen, S. E.; Winder, C.; Sariciftci, N. S.; Denk, P. *Appl Phys Lett* 2002, 80, 1288.
24. Cao, Y.; Yu, G.; Zhang, C.; Menon, R.; Heeger, A. J. *Synth Met* 1997, 87, 171.
25. Bernsten, A.; Croonen, Y.; Liedenbaum, C.; Schoo, H.; Visser, F. J.; Vleggar, J.; Weijer, P. *Opt Mater* 1998, 9, 125.
26. Elschner, A.; Bruder, F.; Heuer, H. W.; Jonas, F.; Karbach, A.; Kirchmeyer, S.; Thurm, S.; Wehrmann, R. *Synth Met* 2000, 111/112, 139.
27. Carter, J. C.; Grizzi, I.; Heeks, S. K.; Lacey, D. J.; Latham, S. G.; May, P. G.; Pa[caron]nos, O. R. D. L.; Pichler, K.; Towns, C. R.; Wittmann, H. F. *Appl Phys Lett* 1997, 71, 34.
28. Aernouts, T.; Geens, W.; Poortmans, J.; Heremans, P.; Borghs, S.; Mertens, R. *Thin Solid Films* 2002, 403, 297.
29. Sariciftci, N. S. *Mater Today* 2004, 25, 39.
30. Lee, R. H.; Lee, Y. Z.; Chao, C. I. *J Appl Polym Sci* 2006, 100, 133.